

Impact of eigenstate thermalization on the route to equilibrium

Jonas Richter,^{*} Jochen Gemmer,[†] and Robin Steinigeweg[‡]
Department of Physics, University of Osnabrück, D-49069 Osnabrück, Germany
 (Dated: May 27, 2019)

The eigenstate thermalization hypothesis (ETH) and the theory of linear response (LRT) are celebrated cornerstones of our understanding of the physics of many-body quantum systems out of equilibrium. While the ETH provides a generic mechanism of thermalization for states arbitrarily far from equilibrium, LRT extends the successful concepts of statistical mechanics to situations close to equilibrium. In our work, we connect these cornerstones to shed light on the route to equilibrium for a class of properly prepared states. We unveil that, if the off-diagonal part of the ETH applies, then the relaxation process can become independent of whether or not a state is close to equilibrium. Moreover, in this case, the dynamics is generated by a single correlation function, i.e., the relaxation function in the context of LRT. Our analytical arguments are illustrated by numerical results for idealized models of random-matrix type and more realistic models of interacting spins on a lattice. Remarkably, our arguments also apply to integrable quantum systems where the diagonal part of the ETH may break down.

Introduction. Both, equilibration and thermalization are omnipresent phenomena in nature. Simple examples in everyday life are a cup of hot coffee which cools down to room temperature, or an inkblot in water which spreads in the entire liquid. Even though the irreversible route to equilibrium occurs in any macroscopic and ordinary situation, the underlying microscopic laws of physics are reversible. In fact, the emergence of phenomenological relaxation from truly microscopic principles such as the Schrödinger equation is not satisfactorily understood up to date. While this fundamental question has a long and fertile history, it has been under intense scrutiny in the last decade [1–5]. This upsurge of interest is also related to the advent of experiments on cold atomic gases [6, 7], the development of sophisticated numerical methods [8], as well as the introduction of fresh theoretical concepts such as quantum typicality of pure states [9–11] and the eigenstate thermalization hypothesis (ETH) [12–14]. In particular, the ETH has become a cornerstone of our understanding of the mere existence of thermalization, but much less is known on the route to equilibrium as such [15–17].

An obvious problem in this context is the absence of an universal approach to the time evolution of quantum many-body systems out of equilibrium. Of course, close to equilibrium, a powerful strategy is provided by the theory of linear response (LRT) [18]. Further away from equilibrium, however, this theory is naturally expected to break down and the dynamics might drastically change for states far from equilibrium. In this respect, our work reports an unexpected and intriguing picture. Following earlier ideas developed by Srednicki [19], we establish a link between LRT and ETH for specific non-equilibrium setups introduced below in detail. We unveil that, if the off-diagonal part of the ETH holds, then the relaxation process can become independent of whether or not a state is close to equilibrium. Moreover, in this case, the time evolution is generated by a single correlation function,

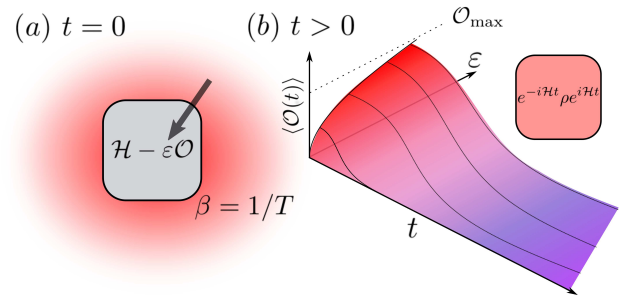


FIG. 1. (Color online) Sketch of the setup. (a) A static force of strength ε gives rise to an additional potential, described by an operator \mathcal{O} . Because of the presence of a heat bath at inverse temperature $\beta = 1/T$, thermalization to the density matrix $\rho = \exp[-\beta(\mathcal{H} - \varepsilon\mathcal{O})]/\mathcal{Z}$ occurs. (b) Static force and heat bath are both removed and ρ undergoes unitary time evolution with respect to \mathcal{H} . We discuss the dependence of the relaxation curve $\langle\mathcal{O}(t)\rangle$ on the perturbation ε outside the regime of small ε .

i.e., the relaxation function in the context of LRT. Our analytical arguments are also confirmed numerically for two different models.

Framework. We will study a physical situation like the one illustrated in Fig. 1. A quantum system, described by a Hamiltonian \mathcal{H} , is affected by an external static force of strength ε . This force gives rise to an additional potential energy, described by an operator \mathcal{O} [20]. Due to the presence of a (macroscopically large and weakly coupled) heat bath at temperature T , thermalization to the density matrix

$$\rho = e^{-\beta(\mathcal{H} - \varepsilon\mathcal{O})}/\mathcal{Z} \quad (1)$$

eventually occurs [18], where $\beta = 1/T$ ($k_B = 1$) denotes the inverse temperature and $\mathcal{Z} = \text{Tr}[e^{-\beta(\mathcal{H} - \varepsilon\mathcal{O})}]$ is the partition function. If the perturbation ε is sufficiently small, the static expectation value $\langle\mathcal{O}(0)\rangle = \text{Tr}[\rho(0)\mathcal{O}]$ is expected to be a linear function of ε , i.e., $\langle\mathcal{O}(0)\rangle =$

$\langle \mathcal{O} \rangle_{\text{eq}} + \varepsilon \chi(0)$, where $\langle \bullet \rangle_{\text{eq}} = \text{Tr}[\rho_{\text{eq}} \bullet]$ is an expectation value with respect to the density matrix $\rho_{\text{eq}} = e^{-\beta \mathcal{H}} / \mathcal{Z}_{\text{eq}}$ and the partition function $\mathcal{Z}_{\text{eq}} = \text{Tr}[e^{-\beta \mathcal{H}}]$. The static susceptibility $\chi(0)$ is given by a Kubo scalar product [18]

$$\chi = \beta(\Delta \mathcal{O}; \mathcal{O}) = \int_0^\beta d\lambda \text{Tr}[\rho_{\text{eq}} \Delta \mathcal{O}(-i\lambda) \mathcal{O}] \quad (2)$$

with $\Delta \mathcal{O} = \mathcal{O} - \langle \mathcal{O} \rangle_{\text{eq}}$ and $\Delta \mathcal{O}(-i\lambda) = e^{\lambda \mathcal{H}} \Delta \mathcal{O} e^{-\lambda \mathcal{H}}$. If ε becomes large enough, this linear relationship breaks down. In particular, given an operator \mathcal{O} with bounded spectrum, $\lim_{\varepsilon \rightarrow \infty} \rho$ is a projector on the eigenstates of \mathcal{O} with the largest eigenvalue \mathcal{O}_{max} . As a consequence, $\lim_{\varepsilon \rightarrow \infty} \langle \mathcal{O}(0) \rangle = \mathcal{O}_{\text{max}}$. Hence, a convenient quantity is the non-equilibrium parameter

$$\zeta(\varepsilon) = \frac{\langle \Delta \mathcal{O}(0) \rangle}{\mathcal{O}_{\text{max}} - \langle \mathcal{O} \rangle_{\text{eq}}}. \quad (3)$$

This quantity becomes $\zeta(\varepsilon) = 0$ for $\varepsilon = 0$ and $\zeta(\varepsilon) = 1$ for $\varepsilon \rightarrow \infty$. While $\zeta(\varepsilon)$ is a natural measure, it might not always be justified to decide solely on this measure if a state is close to or far away from equilibrium [33].

Let us now consider a ‘‘sudden quench’’, where both the external static force and the heat bath are removed at time $t = 0$. Then, at times $t > 0$, the density matrix ρ is no equilibrium state of the remaining Hamiltonian \mathcal{H} and evolves in time according to the von-Neumann equation, $\rho(t) = e^{-i\mathcal{H}t} \rho e^{i\mathcal{H}t}$ ($\hbar = 1$). While this non-equilibrium scenario is generally different to a driven quantum system which unitarily evolves w.r.t. a perturbed Hamiltonian, both setups can, in some cases, be related to each other [21, 33].

The central goal of this paper is to investigate the time-dependent expectation value $\langle \mathcal{O}(t) \rangle = \text{Tr}[\rho(t) \mathcal{O}]$ as a function of the non-equilibrium parameter $\zeta(\varepsilon)$. In the regime of sufficiently small $\zeta(\varepsilon)$, we can certainly expect $\langle \mathcal{O}(t) \rangle = \varepsilon \chi(t)$, where $\chi(t)$ denotes the linear-response relaxation function $\chi(t) = \beta(\Delta \mathcal{O}; \mathcal{O}(t))$ [21, 33]. However, as the theory of linear response is generally restricted to this regime, an intriguing question is: How does the time dependence of $\langle \mathcal{O}(t) \rangle$ change outside this regime? While it is surely challenging to provide a general answer, two of us have recently shown [22] that the time evolution of $\langle \mathcal{O}(t) \rangle$ can become completely independent of $\zeta(\varepsilon)$ if the involved operator \mathcal{O} is binary, i.e., if it only has two different eigenvalues. In this paper, we unveil that such an independence can also occur for other observables, if their matrix structure is in accord with the ETH. This impact of the ETH on the route to equilibrium is the main result of our work and demonstrates its relevance beyond the mere existence of equilibrium.

Illustration: Idealized model. We begin by illustrating our main result for an idealized model of random-matrix type. Its Hamiltonian \mathcal{H}_I is already given in the diagonal form $\mathcal{H}_I = \sum_{n=1}^D E_n |n\rangle \langle n|$, where D is the dimension of the Hilbert space and $|n\rangle$ are the eigenstates of \mathcal{H}_I . The

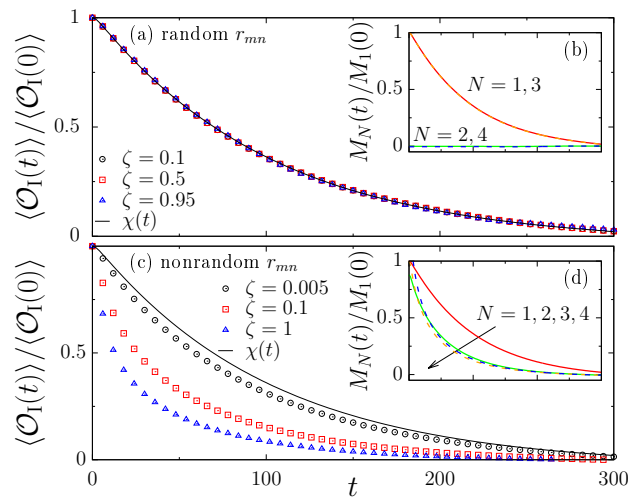


FIG. 2. (Color online) Numerical simulations for the idealized model. Relaxation curve of the normalized expectation value $\langle \mathcal{O}_I(t) \rangle / \langle \mathcal{O}_I(0) \rangle$ for various $\zeta(\varepsilon) = \langle \mathcal{O}_I(0) \rangle / \mathcal{O}_{I,\text{max}}$ as well as the linear-response relaxation function $\chi(t)$. (a) random (Gaussian) r_{mn} and (c) non-random (constant) r_{mn} . Other parameters: $D = 1000$, $\Delta E = 1$, $\gamma = \Delta E/100$, $T = 100$. (b) and (d): $M_N(t) = \text{Tr}[\mathcal{O}_I(t) \mathcal{O}_I^N]$ for exponents $N \leq 4$.

corresponding eigenenergies E_n are simply *chosen* to be equidistant levels $E_n = n \Delta E / D$ in a spectrum of width ΔE , i.e., the density of states $\Omega = D / \Delta E$ is constant. (For a similar model with non-constant Ω , see [33]). In the eigenbasis $|n\rangle$ of \mathcal{H}_I , an observable \mathcal{O}_I is *constructed* as $\mathcal{O}_I = \sum_{m,n=1}^D \mathcal{O}_{I,mn} |m\rangle \langle n|$ with matrix elements

$$\mathcal{O}_{I,mn} = \frac{\Gamma}{\sqrt{\gamma^2 + \omega_{mn}^2}} (1 - \delta_{mn}) r_{mn}, \quad r_{mn} = r_{nm}^*, \quad (4)$$

where the frequency ω_{mn} denotes the energy difference $\omega_{mn} = E_n - E_m$ and γ is a Lorentzian line width. Thus, for $\gamma \ll \Delta E$, \mathcal{O}_I is a banded matrix. Moreover, as δ_{mn} is the Kronecker symbol, $\langle \mathcal{O}_I \rangle_{\text{eq}} = 0$. Within the constraint of a banded matrix, the complex coefficients r_{mn} are free parameters and might be chosen (i) identically or (ii) randomly, e.g., their real and imaginary part might be drawn according to a Gaussian distribution with zero mean. Note that, in the latter case (ii), \mathcal{O}_I is an ideal realization of the ETH ansatz discussed in more detail below. The (in principle irrelevant) prefactor Γ in Eq. (4) is chosen such that $\text{Tr}[\mathcal{O}_I^2] = \text{Tr}[\mathcal{O}_I^4]$.

For the case (ii), we show in Fig. 2 (a) the expectation value $\langle \mathcal{O}_I(t) \rangle$, as resulting for the specific initial state ρ in Eq. (1) and a high temperature T . Remarkably, when $\langle \mathcal{O}_I(t) \rangle$ is normalized to its initial value $\langle \mathcal{O}_I(0) \rangle$, then the relaxation curve is independent of the non-equilibrium parameter $\zeta(\varepsilon) = \langle \mathcal{O}_I(0) \rangle / \mathcal{O}_{I,\text{max}}$ and coincides with the linear-response relaxation function $\chi(t) \propto \text{Tr}[\mathcal{O}_I(t) \mathcal{O}_I]$ in the entire range of $\zeta(\varepsilon) \in]0, 1[$ possible. This numerical simulation illustrates our main result: In *certain* cases, $\chi(t)$ might capture the dynamics at arbitrarily strong

perturbations. But are such cases generic? This question is non-trivial as counterexamples exist. For instance, for the case (i), the relaxation curve in Fig. 2 (c) depends on $\zeta(\varepsilon)$ and agrees with $\chi(t)$ for small $\zeta(\varepsilon) \ll 1$ only.

Analytical arguments and ETH. To work towards an answer to this question, let us discuss the initial state ρ in Eq. (1) for high temperatures T . For such T , we can use the approximation $\rho \approx e^{\beta\varepsilon\mathcal{O}}/\text{Tr}[e^{\beta\varepsilon\mathcal{O}}]$ and a Taylor expansion of this approximation yields

$$\langle \mathcal{O}(t) \rangle \approx \sum_{N=0}^{\infty} \alpha_N(\varepsilon) \text{Tr}[\mathcal{O}(t)\mathcal{O}^N] \quad (5)$$

with some ε -dependent coefficients $\alpha_N(\varepsilon)$. Now, consider the assumption

$$M_N(t) = \text{Tr}[\mathcal{O}(t)\mathcal{O}^N] \begin{cases} \propto \text{Tr}[\mathcal{O}(t)\mathcal{O}], & \text{odd } N \\ = 0, & \text{even } N \end{cases} \quad (6)$$

If this assumption was justified, the expansion in Eq. (5) would directly imply $\langle \mathcal{O}(t) \rangle \propto \text{Tr}[\mathcal{O}(t)\mathcal{O}]$. And in fact, as depicted in Fig. 2 (b), this assumption holds for the idealized model with random r_{mn} . In contrast, as shown in Fig. 2 (d), it breaks down for non-random r_{mn} . Equipped with these prerequisites, we will show that Eq. (6) is closely related to the ETH ansatz [13]

$$\mathcal{O}_{mn} = \mathcal{F}_d(\bar{E}) \delta_{mn} + \Omega(\bar{E})^{-1/2} \mathcal{F}_{od}(\bar{E}, \omega_{mn}) r_{mn}, \quad (7)$$

where $\bar{E} = (E_n + E_m)/2$ and \mathcal{F}_d and \mathcal{F}_{od} are *smooth* functions of their arguments. We will argue that Eq. (6) holds if (qualitatively) \mathcal{F}_{od} varies slowly with \bar{E} and falls off quickly for larger $|\omega_{mn}|$. Furthermore, the diagonal elements \mathcal{O}_{mm} do not need to be smooth functions of \bar{E} as claimed by the ETH, variations that are uncorrelated with the off-diagonal elements \mathcal{O}_{mn} leave Eq. (6) valid. We dub this form of \mathcal{F}_d and \mathcal{F}_{od} the *rigged ETH*. As the proof is quite involved for large exponents N , we restrict ourselves to $N = 2$ and $N = 3$ in the following. For clarity, we also restrict the present consideration to a uniform DOS, $\Omega(\bar{E}) = \text{const.}$, and \mathcal{F}_{od} that are independent of \bar{E} . A full derivation for arbitrary N , as well as more general $\Omega(\bar{E})$ and \mathcal{F}_{od} , can be found in the supplemental material [33].

We start by writing out the correlation function for $N = 2$ explicitly, $\text{Tr}[\mathcal{O}(t)\mathcal{O}^2] = \sum_{a,b,c} \mathcal{O}_{ab}\mathcal{O}_{bc}\mathcal{O}_{ca} e^{i\omega_{ab}t}$, and consider a Fourier component of this correlation function at fixed frequency ω ,

$$\text{Tr}[\mathcal{O}(t)\mathcal{O}^2]_{\omega} = \sum_{\omega_{ab}=\omega} \sum_c \mathcal{O}_{ab}\mathcal{O}_{bc}\mathcal{O}_{ca}. \quad (8)$$

Given the matrix structure in Eq. (7), the biggest part of the addends in the sum are by construction (products of) independent random numbers with zero mean. Thus, to an accuracy set by the law of large numbers, summing the latter yields zero as well. There are, however, index

combinations where not all factors within the addends have vanishing mean, namely, $c = a$. Focusing on these terms, we can write

$$\text{Tr}[\mathcal{O}(t)\mathcal{O}^2]_{\omega} \approx \sum_{\omega_{ab}=\omega} |\mathcal{O}_{ab}|^2 \mathcal{O}_{aa}. \quad (9)$$

While the numbers $|\mathcal{O}_{ab}|^2$ do not have mean zero, we can, without loss of generality, assume that the numbers \mathcal{O}_{aa} have zero mean. Because both numbers are independent stochastic variables [cf. below Eq. (7)], the sum in Eq. (9) becomes $\text{Tr}[\mathcal{O}(t)\mathcal{O}^2]_{\omega} \approx 0$. Since this finding does not depend on ω , we get $\text{Tr}[\mathcal{O}(t)\mathcal{O}^2] \approx 0$, i.e., Eq. (6) for the even case $N = 2$.

Now we turn to $N = 3$. Here, a Fourier component at fixed frequency ω reads

$$\text{Tr}[\mathcal{O}(t)\mathcal{O}^3]_{\omega} = \sum_{\omega_{ab}=\omega} \sum_{c,d} \mathcal{O}_{ab}\mathcal{O}_{bc}\mathcal{O}_{cd}\mathcal{O}_{da}. \quad (10)$$

Again, the contributions of most addends approximately cancel each other upon summation. But again, there are also exceptions, namely, the index combinations $c = a$ or $d = b$. Focusing on these terms, we find

$$\text{Tr}[\mathcal{O}(t)\mathcal{O}^3]_{\omega} \approx \sum_{\omega_{ab}=\omega} |\mathcal{O}_{ab}|^2 \sum_c |\mathcal{O}_{bc}|^2 + |\mathcal{O}_{ac}|^2. \quad (11)$$

To proceed, recall the matrix structure (Eq. (7) and below) and consider the above sum over c without the diagonal elements, i.e., $\sum_{c \neq b} |\mathcal{O}_{bc}|^2 + \sum_{c \neq a} |\mathcal{O}_{ac}|^2$. While these sums do not vanish, they are practically independent of a, b , if $\mathcal{F}_{od}(\bar{E}, \omega_{mn})$ is independent of \bar{E} and vanishes quickly enough for larger $|\omega_{mn}|$. Thus, the respective sums may be replaced by a constant C , i.e., $\sum_c |\mathcal{O}_{bc}|^2 + |\mathcal{O}_{ac}|^2 \approx C + |\mathcal{O}_{aa}|^2 + |\mathcal{O}_{bb}|^2$. The $|\mathcal{O}_{aa(bb)}|^2$ may be split into their mean and variations: $|\mathcal{O}_{aa(bb)}|^2 := \bar{\mathcal{O}}_d^2 + \delta_{a(b)}$. Inserting the above findings into Eq. (11) and exploiting the assumed ‘‘uncorrelatedness’’ of the $\delta_{a(b)}$ with the $|\mathcal{O}_{ab}|^2$ yields $\text{Tr}[\mathcal{O}(t)\mathcal{O}^3]_{\omega} \approx (C + 2\bar{\mathcal{O}}_d^2) \sum_{\omega_{ab}=\omega} |\mathcal{O}_{ab}|^2$. Comparing this to the exact relation $\text{Tr}[\mathcal{O}(t)\mathcal{O}]_{\omega} = \sum_{\omega_{ab}=\omega} |\mathcal{O}_{ab}|^2$ and realizing that all findings are independent of ω , eventually yields $\text{Tr}[\mathcal{O}(t)\mathcal{O}^3] \propto \text{Tr}[\mathcal{O}(t)\mathcal{O}]$, i.e., Eq. (6) for the odd case $N = 3$. Noting that the calculations for $N > 3$ are in principle analogous, we have shown that the assumption in Eq. (6) essentially follows from the ansatz in and below Eq. (7). Hence, we have identified the rigged ETH as the physical mechanism responsible for the numerical observation $\langle \mathcal{O}(t) \rangle \propto \text{Tr}[\mathcal{O}(t)\mathcal{O}]$, even at strong perturbations.

Illustration: Generic quantum many-body systems. Let us now illustrate the relevance of our results to generic quantum many-body systems. A prototype model in this context is the spin-1/2 XXZ chain. We hence consider the Hamiltonian $\mathcal{H}_{\text{XXZ}} = J \sum_{l=1}^L h_l$ (with periodic boundary conditions),

$$h_l = S_l^x S_{l+1}^x + S_l^y S_{l+1}^y + \Delta S_l^z S_{l+1}^z + \Delta' S_l^z S_{l+2}^z, \quad (12)$$

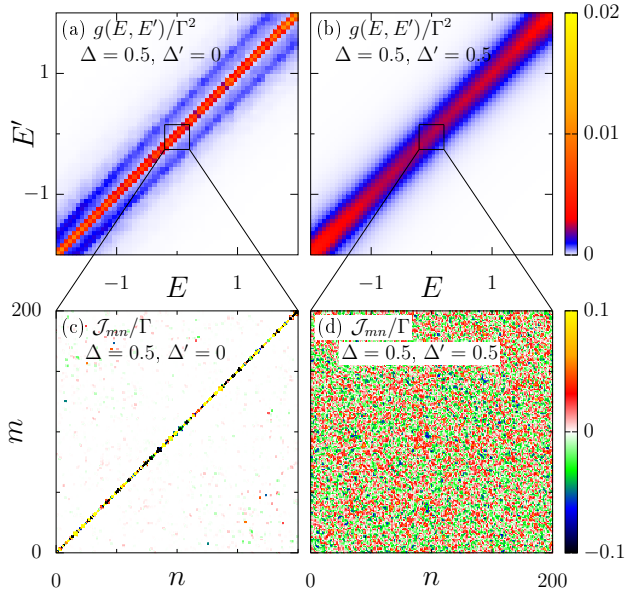


FIG. 3. (Color online) Matrix elements of \mathcal{J} in the eigenbasis of \mathcal{H}_{XXZ} for (a), (c) integrable case ($\Delta' = 0$, $\Delta = 0.5$) and (b), (d) non-integrable case ($\Delta' = 0.5$, $\Delta = 0.5$) in a single symmetry subspace ($S^z = 1$ and $k = 1$). Upper row: Coarse grained structure $g(E, E')$. Lower row: Close-up of 200×200 matrix elements around the diagonal. In all cases, $L = 20$.

where $S_l^{x,y,z}$ are spin-1/2 operators at lattice site l and $J = 1$ is the antiferromagnetic exchange coupling. For vanishing next-nearest-neighbor interaction $\Delta' = 0$, this model is integrable in terms of the Bethe ansatz, whereas integrability is broken for any $\Delta' \neq 0$. As an observable, we choose the well-known spin current [23]

$$\mathcal{J} = \Gamma \sum_{l=1}^L S_l^x S_{l+1}^y - S_{l+1}^x S_l^y, \quad (13)$$

an important quantity in the context of transport. This quantity we study for $\Delta' = 0$ and $\Delta = 0.5$, where it is partially conserved [23, 24], as well as for $\Delta = \Delta' = 0.5$, where it is expected to fully decay. Generally, $\langle \mathcal{J} \rangle_{\text{eq}} = 0$, and again, $\text{Tr}[\mathcal{J}^2] = \text{Tr}[\mathcal{J}^4]$ by a corresponding choice of the prefactor Γ .

The matrix representation of \mathcal{J} in the eigenbasis of \mathcal{H}_{XXZ} is summarized in Fig. 3. The general structure is visualized in Figs. 3 (a) and (b) by the use of a suitable coarse graining according to

$$g(E, E') = \frac{\sum_{mn} |\mathcal{J}_{mn}|^2 D(\bar{E})}{D(E)D(E')}, \quad (14)$$

where the sum runs over matrix elements \mathcal{J}_{nm} in two energy shells of width $2\delta E$, $E_n \in [E - \delta E, E + \delta E]$ and $E_m \in [E' - \delta E, E' + \delta E]$. $D(E)$, $D(E')$, and $D(\bar{E})$ denote the number of states in these energy windows. Note that the coarse grained quantity $g(E, E')$ can be interpreted as

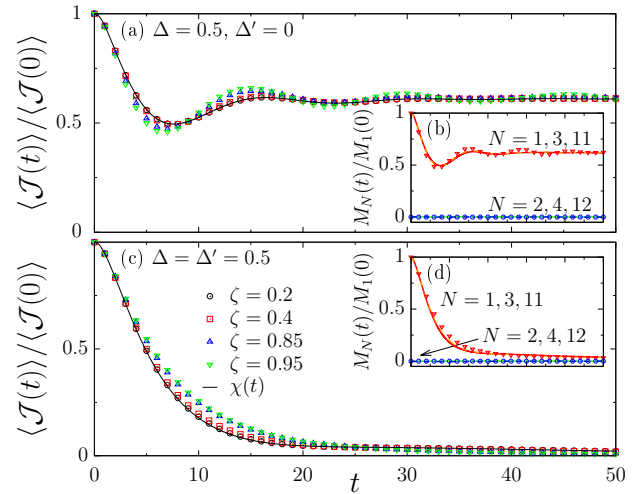


FIG. 4. (Color online) Numerical simulations for the XXZ spin-1/2 chain. Decay curve of the normalized expectation value $\langle \mathcal{J}(t) \rangle / \langle \mathcal{J}(0) \rangle$ for various $\zeta(\varepsilon) = \langle \mathcal{J}(0) \rangle / \mathcal{J}_{\text{max}}$ as well as the linear-response relaxation function $\chi(t)$. (a) integrable case ($\Delta' = 0$, $\Delta = 0.5$) and (c) non-integrable case ($\Delta' = 0.5$, $\Delta = 0.5$). Other parameters: $L = 26$, $T = 100$. (b) and (d): $M_N(t) = \text{Tr}[\mathcal{J}(t)\mathcal{J}^N]$ for exponents $N = 1 - 4$ ($L = 20$) and considerably larger $N = 11, 12$ [34].

a measure of the distribution function \mathcal{F}_{od} in Eq. (7), i.e., $g(E, E') \propto |\mathcal{F}_{\text{od}}(\bar{E}, \omega_{mn})|^2$. Apparently, the situation is very similar for the integrable and non-integrable case: Weight is concentrated around the diagonal and quickly vanishes further away from the diagonal. However, the close-up of matrix elements \mathcal{J}_{mn} in Figs. 3 (c) and (d) unveils clear differences. On the hand, in the integrable case, substantial weight lies directly on the diagonal and the vast majority of all off-diagonal matrix elements are exactly zero, e.g., due to conservation laws. On the other hand, for the non-integrable case, the matrix elements appear to be randomly distributed and it is difficult to recognize any structure at all [25, 26].

Let us finally turn to the dynamics of \mathcal{J} . (For details on the numerics see e.g. Refs. [27–31] and [33]). In Fig. 4 we depict the expectation value $\langle \mathcal{J}(t) \rangle$, as resulting for the specific initial state ρ in Eq. (1) and a high temperature T . When $\langle \mathcal{J}(t) \rangle$ is normalized to its initial value $\langle \mathcal{J}(0) \rangle$ again, then the dynamics does not depend significantly on the non-equilibrium parameter $\zeta(\varepsilon) = \langle \mathcal{J}(0) \rangle / \mathcal{J}_{\text{max}}$ and agrees very well with the linear-response relaxation function $\chi(t) \propto \text{Tr}[\mathcal{J}(t)\mathcal{J}]$ for all $\zeta(\varepsilon) \in [0, 1]$, as shown in Fig. 4 (a) for the integrable case and in Fig. 4 (b) for the non-integrable case. Although the agreement for large $\zeta(\varepsilon)$ is certainly not as perfect as in the idealized model in Fig. 2 (a), it is still convincing. An explanation for the visible deviations might be imperfections in the matrix structure of \mathcal{J} , i.e., small variations compared to the rigged ETH ansatz (cf. Eq. (7) and below). Such variations can manifest themselves

for instance in correlations between the off-diagonal matrix elements, as suggested to exist for local operators [32].

To substantiate that our analytical arguments apply to this model as well, we depict $\text{Tr}[\mathcal{J}(t)\mathcal{J}^N]$ in Figs. 4 (b) and (d). For all exponents N calculated, we confirm that Eq. (6) holds to very good accuracy. While the small deviations for large $\zeta(\varepsilon)$ in Figs. 4 (a) and (c) are presumably caused by high orders in N , Figs. 4 (b) and (d) illustrate that the validity of Eq. (6) approximately persists even for rather large $N = 11, 12$. (For a more detailed discussion of the limitations and physical implications of Eq. (6) see [33]). Finally, we should stress that Eq. (6) is apparently found to apply also in the integrable case, even though the diagonal part of the ETH breaks down.

Conclusion. Given our analytical arguments and our numerical case studies, we conclude that the ETH has impact on the route to equilibrium: If the off-diagonal part of the ETH applies, then the relaxation process can become independent of whether or not the initial state ρ is close to equilibrium. Since we have proven this fact for the specific ρ in Eq. (1) and high temperatures T , promising research directions include other ρ and lower T . Our findings agrees with earlier work by Srednicki [19].

Acknowledgements. This work has been funded by the Deutsche Forschungsgemeinschaft (DFG) - Grants No. 397107022 (GE 1657/3-1), No. 397067869 (STE 2243/3-1), No. 355031190 - within the DFG Research Unit FOR 2692. We sincerely thank the members of FOR 2692 for fruitful discussions.

* jonasrichter@uos.de

† jgemmer@uos.de

‡ rsteinig@uos.de

[1] A. Polkovnikov, K. Sengupta, A. Silva, and M. Vengalattore, *Rev. Mod. Phys.* **83**, 863 (2011).
 [2] J. Eisert, M. Friesdorf, and C. Gogolin, *Nat. Phys.* **11**, 124 (2015).
 [3] R. Nandkishore and D. A. Huse, *Annu. Rev. Condens. Matter Phys.* **6**, 15 (2015).
 [4] C. Gogolin and J. Eisert, *Rep. Prog. Phys.* **79**, 056001 (2016).
 [5] L. D'Alessio, Y. Kafri, A. Polkovnikov, and M. Rigol, *Adv. Phys.* **65**, 239 (2016).
 [6] I. Bloch, *Nat. Phys.* **1**, 23 (2005).
 [7] T. Langen, R. Geiger, and J. Schmiedmayer, *Ann. Rev. Condens. Matter Phys.* **6**, 201 (2015).
 [8] U. Schollwöck, *Rev. Mod. Phys.* **77**, 259 (2005); *Ann. Phys.* **326**, 96 (2011).
 [9] S. Popescu, A. J. Short, and A. Winter, *Nat. Phys.* **2**, 754 (2006).
 [10] S. Goldstein, J. L. Lebowitz, R. Tumulka, and N. Zanghì, *Phys. Rev. Lett.* **96**, 050403 (2006).
 [11] P. Reimann, *Phys. Rev. Lett.* **99**, 160404 (2007).
 [12] J. M. Deutsch, *Phys. Rev. A* **43**, 2046 (1991).

[13] M. Srednicki, *Phys. Rev. E* **50**, 888 (1994).
 [14] M. Rigol, V. Dunjko, and M. Olshanii, *Nature* **452**, 854 (2008).
 [15] E. Khatami, G. Pupillo, M. Srednicki, and M. Rigol, *Phys. Rev. Lett.* **111**, 050403 (2013).
 [16] P. Reimann, *Nat. Commun.* **7**, 10821 (2016).
 [17] L. P. García-Pintos, N. Linden, A. S. L. Malabarba, A. J. Short, and A. Winter, *Phys. Rev. X* **7**, 031027 (2017).
 [18] R. Kubo, M. Toda and, N. Hashitsume, *Statistical Physics II: Nonequilibrium Statistical Mechanics*, Solid-State Sciences **31** (Springer, Berlin, 1991).
 [19] M. Srednicki, *J. Phys. A* **32**, 1163 (1999).
 [20] Not for every observable \mathcal{O} there is a force. See, e.g., R. Zwanzig, *Annu. Rev. Phys. Chem.* **16**, 67 (1965).
 [21] W. Brenig, *Statistical Theory of Heat: Nonequilibrium Phenomena* (Springer, Berlin, 1989).
 [22] J. Richter and R. Steinigeweg, *Phys. Rev. E* **99**, 012114 (2019).
 [23] F. Heidrich-Meisner, A. Honecker, and W. Brenig, *Eur. Phys. J. Spec. Top.* **151**, 135 (2007).
 [24] E. Ilievski, M. Medenjak, T. Prosen, and L. Zadnik, *J. Stat. Mech.* **2016**, 064008 (2016).
 [25] R. Steinigeweg, J. Herbrych, and P. Prelovšek, *Phys. Rev. E* **87**, 012118 (2013).
 [26] W. Beugeling, R. Moessner, and M. Haque, *Phys. Rev. E* **91**, 012144 (2015).
 [27] S. Sugiura and A. Shimizu, *Phys. Rev. Lett.* **108**, 240401 (2012).
 [28] T. A. Elsayed and B. V. Fine, *Phys. Rev. Lett.* **110**, 070404 (2013).
 [29] R. Steinigeweg, J. Gemmer, and W. Brenig, *Phys. Rev. Lett.* **112**, 120601 (2014).
 [30] H. De Raedt and K. Michielsen, *Handbook of Theoretical and Computational Nanotechnology* (American Scientific Publishers, Los Angeles, 2006).
 [31] A. Weiße, G. Wellein, A. Alvermann, and H. Fehske, *Rev. Mod. Phys.* **78**, 275 (2006).
 [32] L. Foini and J. Kurchan, *Phys. Rev. E* **99**, 042139 (2019).
 [33] See supplemental material for details.
 [34] Note that the data for $N = 11$ has been multiplied by a factor to ensure $M_N(0)/M_1(0) = 1$ for easier comparison.

SUPPLEMENTAL MATERIAL

NUMERICAL APPROACH

In our paper, we use numerical methods to calculate expectation values $\langle \mathcal{O}(t) \rangle$. While we use exact diagonalization (ED) to obtain the data for the idealized model in Fig. 1, ED becomes costly for the XXZ spin-1/2 chain because (i) the Hilbert-space dimension $D = 2^L$ grows exponentially with the number of spins L and (ii) the calculation of the expectation value $\langle \mathcal{O}(t) \rangle$ requires ED of both, the pre-quench Hamiltonian $\mathcal{H} - \varepsilon \mathcal{O}$ and the post-quench Hamiltonian \mathcal{H} . Thus, to obtain the data in Figs. 4 (a) and (c), we proceed differently and employ the concept of dynamical quantum typicality as a numerical method [S1–S3]. Specifically, we construct a non-equilibrium pure state of the form [S4]

$$|\psi(0)\rangle = \sqrt{\rho} |\varphi\rangle / \sqrt{\langle \varphi | \rho | \varphi \rangle}, \quad (\text{S1})$$

to mimic the density matrix ρ . Here, the reference pure state $|\varphi\rangle$ is prepared according to the unitary invariant Haar measure, i.e.,

$$|\varphi\rangle = \sum_{k=1}^D c_k |\varphi_k\rangle, \quad (\text{S2})$$

where the real and imaginary part of the coefficients c_k are both drawn from a Gaussian distribution with zero mean and $|\varphi_k\rangle$ denote the states of our working basis, i.e., the Ising basis. Then, the expectation value $\langle \mathcal{O}(t) \rangle$ can be written as [S4]

$$\langle \mathcal{O}(t) \rangle = \langle \psi(t) | \mathcal{O} | \psi(t) \rangle + f(|\phi\rangle) \quad (\text{S3})$$

with the statistical error $f(|\phi\rangle) \propto 1/\sqrt{D}$ in the limit of high temperatures $\beta \rightarrow 0$. Thus, $f(|\phi\rangle)$ is negligibly small for medium-sized lattice sizes L already. The main advantage of Eq. (S3) stems from the fact, that the action of the exponentials $e^{-\beta(\mathcal{H}-\varepsilon\mathcal{O})}$ and $e^{-i\mathcal{H}t}$ can be conveniently evaluated by a forward propagation of pure states in imaginary time β or real time t . For this forward propagation, various sophisticated methods can be used, e.g., Trotter decompositions [S5] or Chebyshev polynomials [S6]. In the present paper, it is sufficient to apply a fourth-order Runge-Kutta scheme [S2, S3] with a small time step δt . Since this scheme does not require ED and the involved operators usually feature a sparse matrix representation, we can easily calculate data for $L = 26$ sites, as done in Figs. 4 (a) and (c).

RELATION TO OTHER NON-EQUILIBRIUM SCENARIOS

In the main part of this paper, we have studied the relaxation dynamics $\langle \mathcal{O}(t) \rangle$, as resulting from an initial

state $\rho = \exp[-\beta(\mathcal{H} - \varepsilon\mathcal{O})]/\mathcal{Z}$. While this setup might not be the most common preparation scheme, it can be related to other non-equilibrium scenarios in the regime of linear response, i.e., small perturbations ε . To this end, let us consider a thermal initial state $\rho(-\infty) = \rho_{\text{eq}}$ and an external field which is turned on at $t = -\infty$ and switched off at $t = 0$, i.e.,

$$\mathcal{H}(t) = \begin{cases} \mathcal{H} - \varepsilon(t) \mathcal{O}, & t < 0 \\ \mathcal{H}, & t \geq 0 \end{cases}. \quad (\text{S4})$$

In this case, the expectation value $\langle \mathcal{O}(t) \rangle$ can be written as

$$\langle \mathcal{O}(t) \rangle = \int_{-\infty}^0 dt' \phi(t-t') \varepsilon(t'), \quad (\text{S5})$$

where we have introduced the *response function* $\phi(t)$. If we now assume a weak and quasi-static external field $\varepsilon(t) \approx \varepsilon$, then this setup translates into the relaxation experiment considered in the main part of this paper. Specifically, the relaxation function $\chi(t)$ and the response function $\phi(t) = -\beta(\Delta\mathcal{O}; \dot{\mathcal{O}}(t))$ can be related according to [S7]

$$\chi(t) = \Theta(t) \left[\chi(0) - \int_0^t dt' \phi(t') \right]. \quad (\text{S6})$$

Hence, knowledge of either $\chi(t)$ or $\phi(t)$ is sufficient to describe both scenarios.

CHARACTERIZATION OF INITIAL STATES

In the main text, we have investigated initial states $\rho = \exp[-\beta(\mathcal{H} - \varepsilon\mathcal{O})]/\mathcal{Z}$ and argued that the tuning of the perturbation ε allows for a preparation of ρ close to as well as far away from equilibrium. While it seems to be natural that a ρ with larger ε has to be considered as further away from equilibrium, it is still somewhat ambiguous without reasonable criteria to characterize ρ as *close to* or *far away from* equilibrium. In the following, let us discuss this point in more detail.

As already mentioned, the initial expectation value $\langle \mathcal{O}(0) \rangle$ can be used as a natural criterion to decide whether a state is far away from equilibrium. Recall that $\langle \mathcal{O}(0) \rangle$ is limited by the maximum eigenvalue \mathcal{O}_{max} of the operator \mathcal{O} . Therefore, in the main text, we have defined the relative deviation from equilibrium

$$\zeta(\varepsilon) = \frac{\langle \Delta\mathcal{O}(0) \rangle}{\mathcal{O}_{\text{max}} - \langle \mathcal{O}_{\text{eq}} \rangle}, \quad (\text{S7})$$

with $\langle \mathcal{O} \rangle_{\text{eq}} = 0$ in the two case studies. Thus, one might call a state ρ close to equilibrium if $\zeta \approx 0$ and far from equilibrium if $\zeta \approx 1$.

Let us discuss the dependence of $\zeta(\varepsilon)$ on the strength of the perturbation ε . In Figs. S1 (a), (c), and (e), $\zeta(\varepsilon)$

is shown for the idealized operator \mathcal{O}_I with random and non-random r_{mn} as well as for the spin-current operator \mathcal{J} . In all cases, the temperature is set to $T = 100$. Since the static curves at such high T practically do not depend on \mathcal{H} , it is sufficient to show $\langle \mathcal{J}(0) \rangle$ only for one choice of the anisotropies Δ and Δ' . For illustration, Figs. S1 (a), (c), and (e) indicate those values of ε which are chosen in the main text to study the actual dynamics. While we observe that, for all observables, $\zeta(\varepsilon)$ monotonically increases with increasing ε until it eventually saturates at $\langle \mathcal{O}(0) \rangle = \mathcal{O}_{\max}$, we also find that the values of ε to reach this maximum significantly depend on the specific operator. The latter fact becomes clear if one takes into account the different scaling of the horizontal ε axis for the three operators. Apparently, a specific value of ε may cause a large response for one operator but only a small response for another operator. Thus, compared to the bare value of ε , the parameter $\zeta(\varepsilon)$ yields much better information on whether ρ is close to or far away from equilibrium. However, in addition to $\zeta(\varepsilon)$, it might be even more insightful to consider the whole spectrum and analyze the density of states (DOS) of the respective operators.

The DOS of some operator \mathcal{O} is defined as

$$\Omega(E) = \sum_{n=1}^D \delta(E - O_n), \quad (\text{S8})$$

where the O_n denote the eigenvalues of \mathcal{O} . Even though it is straightforward to calculate $\Omega(E)$ by means of exact diagonalization, we additionally use a typicality approach [S8] to evaluate the DOS of \mathcal{J} . Specifically, we exploit

$$\text{Tr}[e^{-i\mathcal{O}t}] \approx \langle \Phi | e^{-i\mathcal{O}t} | \Phi \rangle \quad (\text{S9})$$

for a pure state $|\Phi\rangle$ drawn at random. Using the integral representation of the δ -function,

$$\delta(E - O_n) = \frac{1}{2\pi} \int_{-\infty}^{\infty} e^{it(E - O_n)}, \quad (\text{S10})$$

we then have

$$\Omega(E) \approx C \int_{-\Theta}^{\Theta} dt e^{i\mathcal{O}t} \langle \Phi | e^{-i\mathcal{O}t} | \Phi \rangle, \quad (\text{S11})$$

where C is a normalization constant and the spectral resolution δE depends on the cutoff time, $\delta E = \pi/\Theta$. In Figs. S1 (b), (d) and (f) we depict the DOS for \mathcal{O}_I with random and non-random r_{mn} and for \mathcal{J} . Also in the case of $\Omega(E)$, we observe clear differences between the three operators. First, for \mathcal{O}_I with random r_{mn} , $\Omega(E)$ follows the well-known semi-circle from random matrix theory and second, for \mathcal{O}_I with non-random r_{mn} , $\Omega(E)$ exhibits a strong degeneracy around $E = 0$ and a long tail up to a quite large maximum eigenvalue \mathcal{O}_{\max} . Third, in case of \mathcal{J} , $\Omega(E)$ has a Gaussian shape.

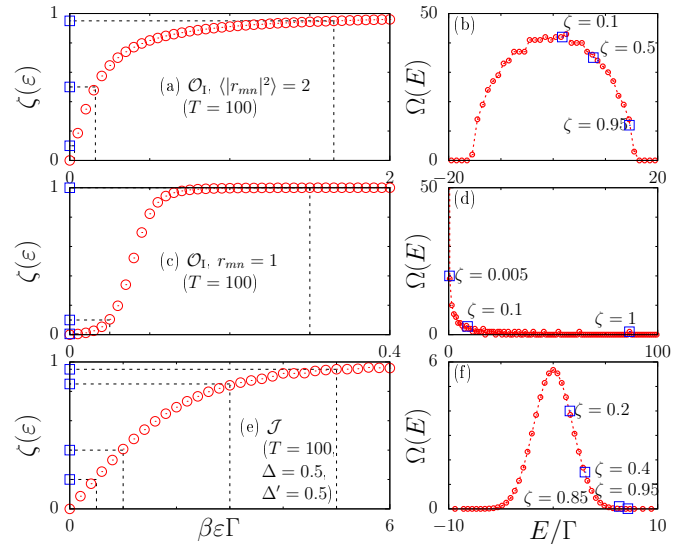


FIG. S1. (Color online) (a), (c), and (e): Initial expectation value $\zeta = \langle \mathcal{O}(0) \rangle / \mathcal{O}_{\max}$ versus perturbation ε for $\mathcal{O} = \mathcal{O}_I$ with random and non-random r_{mn} as well as $\mathcal{O} = \mathcal{J}$. The lines indicate those values of ε which are used in the main text to study the actual dynamics. The squares indicate the corresponding values of $\zeta(\varepsilon)$. (b), (d), and (f): DOS for the same three operators. The location of $\zeta(\varepsilon)$ is depicted again by squares.

As an orientation, we indicate also in Figs. S1 (b), (d) and (f) the location of the initial states from the text with their different values of $\zeta(\varepsilon)$. While this location is roughly at the maximum of $\Omega(E)$ for small $\zeta(\varepsilon)$, it shifts to the borders of the spectrum as $\zeta(\varepsilon)$ is increased to larger values. In particular, for $\zeta(\varepsilon) \approx 1$, we find that the initial states are located in a region with a very low DOS and it is certainly justified to consider such states as far from equilibrium. Hence, our choices of $\zeta(\varepsilon)$ cover the whole range of initial states close to and far away from equilibrium.

RANDOM-MATRIX MODEL WITH NON-CONSTANT DENSITY OF STATES

In the context of Fig. 2, we considered a random-matrix model in order to demonstrate the validity of our analytical results for an ideal realization of the ETH Ansatz given in and below Eq. (7). In this case, the Hamiltonian \mathcal{H}_I was chosen with equidistant energy levels, i.e., a constant density of states $\Omega = \text{const}$. Here, we additionally study the non-equilibrium dynamics of a similar random-matrix model with non-constant Ω . Specifically, the eigenenergies E_n of \mathcal{H}_I are now randomly drawn from an exponential probability distribution in the interval $E_n \in [0, 1]$. Thus, the density of states in this interval is approximately given by

$$\Omega(E) \propto e^{\beta' E}. \quad (\text{S12})$$

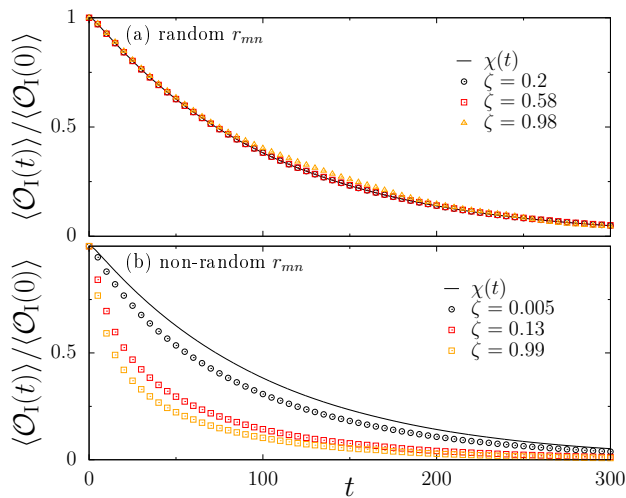


FIG. S2. (Color online) Numerical simulations for the random-matrix model with exponential density of states. Relaxation curve of the normalized expectation value $\langle \mathcal{O}_I(t) \rangle / \langle \mathcal{O}_I(0) \rangle$ for various $\zeta(\varepsilon) = \langle \mathcal{O}_I(0) \rangle / \mathcal{O}_{I,\max}$ as well as the linear-response relaxation function $\chi(t)$. (a) random (Gaussian) r_{mn} and (b) non-random (constant) r_{mn} . Other parameters: $D = 2000$, $\Delta E = 1$, $\gamma = \Delta E / 100$, $T = 100$.

We here choose $\beta' = 1$ such that $\Omega(1) \approx e \cdot \Omega(0)$, and $\Omega(E)$ significantly deviates from a constant. The respective observable \mathcal{O}_I is again constructed as described in Eq. (4), with random or non-random elements r_{mn} and Lorentzian damping. However, due to the non-constant density of states, the matrix elements with mean energy \bar{E} are now additionally multiplied by the factor $\Omega(\bar{E})^{-1/2} = e^{-\beta' \bar{E}/2}$, cf. Eq. (7).

In Fig. S2 we depict the non-equilibrium dynamics for the random-matrix model with non-constant density of states. Generally, the results are very similar compared to the previous model studied in the context of Fig. 2. In particular, for random matrix elements r_{mn} , the non-equilibrium dynamics $\langle \mathcal{O}_I(t) \rangle$ is essentially proportional to the linear response relaxation function in the entire regime $\zeta \in]0, 1]$. This behavior clearly breaks down if the r_{mn} are non-random, cf. Fig. S2 (b). While there are some small deviations in Fig. S2 (a) for the very large $\zeta = 0.98$, let us emphasize that our derivations generally rely on the law of large numbers, and, therefore, the results in Fig. S2 are still rather convincing in view of the small matrix dimension $D = 2000$. We elaborate in detail on the reasons for (and the limits of) the good agreement in Fig. S2 (a) in the last section of the supplemental material. However, important features for the occurrence of this agreement are a density of states that is well described by an exponential over a wide energy range and a decay of $\langle \mathcal{O}(t) \rangle$ that is rather slow on a timescale set by the inverse of the above wide energy range.

IMPLICATIONS OF THE MAIN ASSUMPTION ON PHYSICALLY RELEVANT QUANTITIES

While the validity of Eq. (6) from the main text is clearly mathematically nontrivial for any $N > 1$, it is not evident whether or not a validity for, say, $N = 5$ entails a physically relevant result. Specifically, if the number of particles (spins) N_p increases, does the minimum N in Eq. (6), which is required to yield a physically meaningful result, increase as well? And if so how? Before elaborating on this question we anticipate a brief answer: Let the spectrum of the observable \mathcal{O} be Gaussian, with a standard deviation $\sigma_{\mathcal{O}}$. Then, the validity of Eq. (6) up to a maximum exponent $N = f$ renders

$$\langle \mathcal{O}(t) \rangle \propto \text{Tr}[\mathcal{O}(t)\mathcal{O}(0)] \quad (\text{S13})$$

valid, for initial states

$$\rho \propto \exp(\beta\varepsilon\mathcal{O}), \quad (\text{S14})$$

and initial values $\langle \mathcal{O}(0) \rangle$ which are on the order of $f\sigma_{\mathcal{O}}$. Hence, even if one finds that f does not scale with N_p at all, but assumes a value like, e.g., $N = 5$, this already implies the validity of Eq. (S13) for the largest part of the spectrum. It implies furthermore a validity of Eq. (S13) which is, loosely speaking, five times larger than what linear response alone accounts for. However, an f that does not scale with N_p (and is not very large ($\gg 1$) already for small systems) does not entail a validity of Eq. (S13) in the “large-deviation regime”, i.e., in the outer tails of the spectrum of \mathcal{O} . Note that a principal consideration on the expected f for a given observable and Hamiltonian is provided in the next section.

We now embark on a detailed justification of the above statement. In essence, Eq. (S13) will be valid if the following truncation of the Taylor-series approximates the respective exponential well (we set $\alpha = \beta\varepsilon$ in the following),

$$e^{\alpha\mathcal{O}} \approx \sum_n^{n=f} \frac{1}{n!} (\alpha\mathcal{O})^n. \quad (\text{S15})$$

The question now is: how large may α, \mathcal{O} maximally be for a given f to render Eq. (S15) valid? The weight in the addends of a Taylor-series is Poisson distributed. If $\alpha\mathcal{O}$ was a number, the expectation value and standard deviation of the respective “term distribution” would accordingly (see standard math textbooks) read

$$\bar{n} = \alpha\mathcal{O}, \quad \sigma_n = \sqrt{\alpha\mathcal{O}}. \quad (\text{S16})$$

Thus at

$$\alpha\mathcal{O} \leq \frac{f}{c_1}, \quad (\text{S17})$$

with c_1 a bit larger than unity, Eq. (S15) will be valid to good accuracy for $f \gg 1$. For small f , choosing $c_1 = 10$

will suffice. However, $\alpha\mathcal{O}$ is not a number. Thus we aim at making Eq. (S15) valid for most of the spectrum of \mathcal{O} . Let $E_{\mathcal{O}}$ be a (positive) number such that a big percentage of the eigenvalues of \mathcal{O} falls into $[-E_{\mathcal{O}}, E_{\mathcal{O}}]$. Then, a mathematically admissible version of Eq. (S17) reads

$$\alpha E_{\mathcal{O}} \leq \frac{f}{c_1}. \quad (\text{S18})$$

Let us now think of \mathcal{O} as a standard ‘‘local’’ observable. The widths of the spectra of such observables usually scale as $\propto \sqrt{N_p}$ and the spectra are more or less Gaussian. Thus $E_{\mathcal{O}}$ may be chosen as $E_{\mathcal{O}} = c_2 \sqrt{N_p}$, with c_2 sufficiently large, see below. This makes Eq. (S18) read $\alpha c_2 \sqrt{N_p} \leq \frac{f}{c_1}$, i.e., the regime of α for which Eq. (S15) holds is limited as

$$\alpha \leq \frac{f}{c_1 c_2 \sqrt{N_p}}. \quad (\text{S19})$$

Now we analyze the largest initial expectation value, $\langle \mathcal{O}(0) \rangle$, that may be reached based on the above α , i.e., a given f . Let \mathcal{O} have for simplicity a continuous spectrum $s(x)$. As argued below Eq. (S18), s is expected to be approximately Gaussian with a standard deviation which may be written as $\sigma_{\mathcal{O}} = c_3 \sqrt{N_p}$. Hence we get $s(x) \propto \exp(-\frac{x^2}{2c_3^2 N_p})$. Now we come back to the above choice of c_2 . If we require Eq. (S15) to hold for, e.g., 99.73% of all eigenstates of \mathcal{O} , then we have to choose $c_2 = 3 \cdot c_3$. Let $p(x)$ be the probability to find the observable \mathcal{O} initially at x . The most ‘‘dislocated’’ $p(x)$ we can faithfully generate with some given f in an initial state of the form (S14) is:

$$p(x) \propto e^{-\frac{x^2}{2c_3^2 N_p}} e^{-\frac{f}{c_1 c_2 \sqrt{N_p}}} \propto e^{-\frac{1}{2c_3^2 N_p} (x - \frac{f c_3 \sqrt{N_p}}{c_1 c_2})^2}. \quad (\text{S20})$$

The mean value (and the maximum) of this distribution is

$$\langle \mathcal{O}(0) \rangle = \frac{f c_3^2 \sqrt{N_p}}{c_1 c_2}. \quad (\text{S21})$$

Thus, $\langle \mathcal{O}(0) \rangle$ scaled against $\sigma_{\mathcal{O}}$ gives

$$\frac{\langle \mathcal{O}(0) \rangle}{\sigma_{\mathcal{O}}} = \frac{f c_3}{c_1 c_2}, \quad (\text{S22})$$

or, imposing the above relation of c_2, c_3 ,

$$\frac{\langle \mathcal{O}(0) \rangle}{\sigma_{\mathcal{O}}} = \frac{f}{3 \cdot c_1}. \quad (\text{S23})$$

Now comes the crucial point: This relation is entirely independent of N_p . Hence the validity of Eq. (6) entails a physically meaningful result even if the maximum N for which it holds does not scale with N_p at all. Very roughly speaking (setting c_1 to unity), this means that

the validity of Eq. (6) up to some $N = f$ ensures that Eq. (S13) will hold up to initial values of \mathcal{O} that are $f/3$ -times larger than the standard deviation of \mathcal{O} , regardless of the size of the system. Note that a scaling like, e.g., $f \propto \sqrt{N_p}$ would already address the ‘‘large-deviation regime’’, i.e., a validity of (S13) for initial values of \mathcal{O} that are far out in the tails of the spectrum of \mathcal{O} .

Tr[$\mathcal{O}(t)\mathcal{O}^N$] FOR ARBITRARY N

To begin with, consider a Fourier component of Tr[$\mathcal{O}(t)\mathcal{O}^N$] at fixed frequency ω :

$$\text{Tr}[\mathcal{O}(t)\mathcal{O}^N]_{\omega} = \sum_{\omega_{ab}=\omega} \mathcal{O}_{ab} \cdot \sum_{i,j,k,l,\dots} (\mathcal{O}_{bi}\mathcal{O}_{ij} \cdots \mathcal{O}_{kl}\mathcal{O}_{la}), \quad (\text{S24})$$

where the second sum is just an expanded representation of $(\mathcal{O}^N)_{ba}$ and the first sum runs over all indices a, b with $E_b - E_a = \omega_{ab}$. Since \mathcal{O} is essentially a random matrix [see Eq. (7)], most addends in Eq. (S24) are products of independent random numbers. As such they will be random numbers themselves, with random phases (or signs, in case \mathcal{O} should be real). Hence, to an accuracy set by the law of large numbers, these addends will sum up to zero. However, there are index combinations for which the respective addends are not just products of independent random numbers but necessarily real and positive. (These are also the only addends that would ‘‘survive’’ an averaging of Eq. (S24) over concrete implementations of \mathcal{O} .) For the remainder we focus exclusively on these addends.

A first necessary, but by no means sufficient condition on the indices to render the respective addends surely positive, may be stated as follows: The indices of one of the \mathcal{O} ’s in the second sum on the r.h.s. of Eq. (S24) must be chosen as \mathcal{O}_{ba} . A second necessary but not sufficient condition on ‘‘surely positive’’ addends is that the remaining products of \mathcal{O} ’s must consist of even numbers of factors (elements of \mathcal{O}). This means that the addends of the second sum on the r.h.s. of Eq. (S24) must be of the following form

$$\underbrace{\mathcal{O}_{bi} \cdots \mathcal{O}_{jb}}_{N-P-1} \mathcal{O}_{ba} \underbrace{\mathcal{O}_{ak} \cdots \mathcal{O}_{la}}_P, \quad (\text{S25})$$

where the expressions below the underbraces indicate the respective numbers of multiplied elements of \mathcal{O} , $N-P-1$ and P are even integers. Since $N-P-1$ and P both must be even, it follows that N must be odd. This already establishes the lower line of Eq. (6). However, without any further condition on the remaining indices i, j, k, l , etc., the products given in (S25) are not yet surely positive. A third condition which (together with the previous two conditions) is sufficient for sure positiveness of the addends in Eq. (S24) is that the remaining indices of the

underbraced products must all be “paired”. This means that if such a product has some factor \mathcal{O}_{ij} it must *also* have the factor \mathcal{O}_{ji} such as to form $|\mathcal{O}_{ji}|^2$. (This principle also underlies the first and second necessary condition.) Such a pairing can be achieved in many ways. For example, for the first product in (S25) some of them may be schematically written as

$$\mathcal{O}_{bi}\mathcal{O}_{ij}\mathcal{O}_{jk}\cdots\mathcal{O}_{kj}\mathcal{O}_{ji}\mathcal{O}_{ib} , \quad (\text{S26})$$

$$\mathcal{O}_{bi}\mathcal{O}_{ib}\mathcal{O}_{bj}\mathcal{O}_{ji}\cdots\mathcal{O}_{ij}\mathcal{O}_{jb} , \quad (\text{S27})$$

$$\mathcal{O}_{bi}\mathcal{O}_{ij}\cdots\mathcal{O}_{ji}\mathcal{O}_{ib}\mathcal{O}_{bl}\mathcal{O}_{lb} . \quad (\text{S28})$$

The “building blocks” of these paired index combinations are sequences of indices with a mirror symmetry, such that the second part repeats the first part in reversed order, i.e., $b, i, j, k, \dots, k, j, i, b$. The first example, i.e., (S26), consists only of one single building block. The second and the third example, i.e., (S27) and (S28), consist of two building blocks of different lengths in different order [(S27): short first; (S28): long first]. For large $N - P - 1$ and respectively P , there are very many possibilities to create different building blocks of different lengths and arrange them in different orders. It is very hard to organize these possibilities in a reasonable manner. Fortunately, we do not need to do this here. To proceed further, we first make an assumption on a property of the building blocks and show that the validity of Eq. (6) may be inferred from this assumption. Then we justify the assumption, thereby elucidating its limitations. In order to clearly formulate the assumption we consider a “summed building block”, $f(c, Q)$, given as

$$f(c, Q) := \sum_{i,j,k,l,\dots} \mathcal{O}_{ci}\mathcal{O}_{ij}\mathcal{O}_{jk}\cdots\mathcal{O}_{kj}\mathcal{O}_{ji}\mathcal{O}_{ic} , \quad (\text{S29})$$

where Q (integer, even) indicates the numbers of \mathcal{O} 's in the addends. Note that the summation is over all indices except for the “end index”, in this case c . Now, the assumption is as follows: Assume that the $f(c, Q)$ are actually independent of c , regardless of Q . To this end, consider a sum over the terms in (S25) as

$$g(a, b, N, P) := \left(\sum_{i,\dots,j} \underbrace{\mathcal{O}_{bi}\cdots\mathcal{O}_{jb}}_{N-P-1} \right) \mathcal{O}_{ba} \left(\sum_{k,\dots,l} \underbrace{\mathcal{O}_{ak}\cdots\mathcal{O}_{la}}_P \right) . \quad (\text{S30})$$

Note that all relevant contributions of the second sum in Eq. (S24), i.e., to $(\mathcal{O}^N)_{ba}$, are of the form $g(a, b, N, P)$. Since the paired contributions to the two sums of $g(a, b, N, P)$ all consist of summed building blocks of the form $f(c, Q)$, it follows that, given the above assumption on the $f(c, Q)$, the two sums themselves do not depend on a, b respectively. Hence $g(a, b, N, P)$ is of the approximate (up to unpaired contributions) form

$$g(a, b, N, P) \approx C(N, P) \cdot \mathcal{O}_{ba} , \quad (\text{S31})$$

where $C(N, P)$ is a constant w.r.t. a, b . Since, as mentioned below Eq. (S30), $(\mathcal{O}^N)_{ba}$ is a sum of $g(a, b, N, P)$'s over the allowed P , it follows that

$$(\mathcal{O}^N)_{ba} \propto \mathcal{O}_{ba} + \text{non-surely pos. contribution} . \quad (\text{S32})$$

If Eq. (S32) holds, then Eq. (6) from the main text also holds, in the “law of large numbers sense” described below Eq. (S24).

Now, the remaining crucial question is if and to what extent $f(c, Q)$ is indeed independent of c . In order to analyze this, consider a version of the ETH ansatz as suggested, e.g., in [S9] and given by Eq. (7) with some additional conditions on the functions $\Omega(E)$, $\mathcal{F}_{\text{od}}(\bar{E}, \omega)$ contained in that ansatz (“rigged ETH”). Let $\Omega(E)$ be a function that is piecewise nicely described by exponentials, i.e., $\Omega(E) \approx \Omega_0 \exp(\beta E)$. Let the energy intervals to which the respective mono-exponential form applies be not too small fractions of the full width of the energy spectrum, such as, e.g., for a Gaussian DOS. Let furthermore $\mathcal{F}_{\text{od}}(\bar{E}, \omega)$ be approximately independent of \bar{E} within such energy intervals, i.e., $\mathcal{F}_{\text{od}}(\bar{E}, \omega) \approx \mathcal{F}_{\text{od}}(\omega)$ for all \bar{E} from an interval. Eventually $\mathcal{F}_{\text{od}}(\omega)$ must be suitably narrow: Let $\delta\omega$ be the typical width of $\mathcal{F}_{\text{od}}(\omega)$. Then we require $Q \cdot \delta\omega$ to be still smaller than the interval on which the DOS is mono-exponential. We dub these specifications of Eq. (7) the *rigged ETH*. This eventually sets a limit to the maximum power of \mathcal{O} , i.e., N . As one last brutal simplification we set $\mathcal{F}_{\text{d}}(\bar{E}) = 0$. This condition can be relaxed substantially as we will demonstrate in a forthcoming publication. Here, we employ it for simplicity and clarity of presentation.

Equipped with these specifications, we now embark on a concrete calculation of $f(c, Q)$,

$$f(c, Q) = \sum_{i,j,\dots,k,l} |\mathcal{O}_{ci}|^2 |\mathcal{O}_{ij}|^2 \cdots |\mathcal{O}_{kl}|^2 . \quad (\text{S33})$$

We plug Eq. (7) together with the aforementioned specifications into Eq. (S33). Furthermore, we entirely rely on the law of large numbers, i.e., we replace $|r_{ij}|^2 \rightarrow 1$. This yields

$$f(c, Q) \approx \sum_{i,j,\dots,k,l} \Omega_0^{-Q} e^{-\frac{\beta}{2}(E_c + 2E_i + \cdots + 2E_k + E_l)} \cdot \mathcal{F}_{\text{od}}^2(E_c - E_i) \mathcal{F}_{\text{od}}^2(E_i - E_j) \cdots \mathcal{F}_{\text{od}}^2(E_k - E_l) . \quad (\text{S34})$$

Now, we go from sums to integrals, essentially by plugging in the respective DOS's

$$f(c, Q) \approx \int \Omega_0^{-Q} e^{-\frac{\beta}{2}(E_c + 2E_1 + \cdots + 2E_{L-1} + E_L)} \cdot \mathcal{F}_{\text{od}}^2(E_c - E_1) \mathcal{F}_{\text{od}}^2(E_1 - E_2) \cdots \mathcal{F}_{\text{od}}^2(E_{Q-1} - E_Q) \cdot \Omega_0^Q e^{\beta(E_1 + E_2 + \cdots + E_{Q-1} + E_Q)} dE_1 dE_2 \cdots dE_Q . \quad (\text{S35})$$

Here, we off course heavily rely on the above specifications. A closer look reveals that most of the DOS's from

the ETH ansatz cancel nicely with the DOS's from the integrations:

$$f(c, Q) \approx e^{-\frac{\beta}{2}E_c} \int e^{\frac{\beta}{2}E_Q} \cdot \mathcal{F}_{\text{od}}^2(E_c - E_1) \mathcal{F}_{\text{od}}^2(E_1 - E_2) \cdots \mathcal{F}_{\text{od}}^2(E_{Q-1} - E_Q) \cdot dE_1 dE_2 \cdots dE_Q . \quad (\text{S36})$$

We apply the following linear change of variables,

$$\begin{aligned} E_1, E_2 \cdots E_{Q-1}, E_Q & \quad (\text{S37}) \\ \rightarrow \\ \omega_1 := E_c - E_1, \omega_2 := E_1 - E_2, \cdots \\ \omega_Q := E_{Q-1} - E_Q , \end{aligned}$$

which features a Jacobian determinant which equals unity. (The matrix has lower triangle form and the diagonal elements are all -1 .) Furthermore, we realize

$$E_Q = E_c - \sum_{i=1}^Q \omega_i . \quad (\text{S38})$$

Thus, in the new variables the integral from Eq. (S36) reads

$$f(c, Q) \approx \int e^{-\frac{\beta}{2} \sum_{i=1}^Q \omega_i} \cdot \mathcal{F}_{\text{od}}^2(\omega_1) \mathcal{F}_{\text{od}}^2(\omega_2) \cdots \mathcal{F}_{\text{od}}^2(\omega_Q) \cdot d\omega_1 d\omega_2 \cdots d\omega_Q = \left(\int e^{-\frac{\beta\omega}{2}} \mathcal{F}_{\text{od}}^2(\omega) d\omega \right)^Q . \quad (\text{S39})$$

Displayed in this form, $f(c, Q)$ is manifestly independent of c . This completes the justification for the assumption made before Eq. (S30).

Thus, to sum up, the validity of Eq. (6) from the main text can be expected, more or less pronounced, if the following specifications, in addition to the standard ETH

ansatz, apply: (i) DOS's that are in accord with exponentials over substantial energy ranges, (ii) $\mathcal{F}_{\text{od}}(\bar{E}, \omega)$'s that vary slowly or/and weakly with \bar{E} , (iii) $\mathcal{F}_{\text{od}}(\bar{E}, \omega)$'s that are narrow in ω direction, (iv) small N . This appears to be in accord with the numerical findings: For the idealized random-matrix model, (i)-(iii) apply very well. Thus, the above arguments apply even for large N or exponential initial states featuring large exponents. For the lattice spin-model, (i)-(iii) apply also, but not as strictly as for the random-matrix model. Thus, Eq. (6) from the main text breaks down for exponential initial states featuring large exponents.

* jonasrichter@uos.de

† jgemmer@uos.de

‡ rsteinig@uos.de

- [S1] S. Sugiura and A. Shimizu, Phys. Rev. Lett. **108**, 240401 (2012).
- [S2] T. A. Elsayed and B. V. Fine, Phys. Rev. Lett. **110**, 070404 (2013).
- [S3] R. Steinigeweg, J. Gemmer, and W. Brenig, Phys. Rev. Lett. **112**, 120601 (2014).
- [S4] J. Richter and R. Steinigeweg, Phys. Rev. E **99**, 012114 (2019).
- [S5] H. De Raedt and K. Michielsen, *Handbook of Theoretical and Computational Nanotechnology* (American Scientific Publishers, Los Angeles, 2006).
- [S6] A. Weiße, G. Wellein, A. Alvermann, and H. Fehske, Rev. Mod. Phys. **78**, 275 (2006).
- [S7] W. Brenig, *Statistical Theory of Heat: Nonequilibrium Phenomena* (Springer, Berlin, 1989).
- [S8] A. Hams and H. De Raedt, Phys. Rev. E **62**, 4365 (2000).
- [S9] M. Srednicki, J. Phys. A **32**, 1163 (1999).